Pengpeng Zhang
Department of Mechanical and Industrial Engineering,
Louisiana State University,
Baton Rouge, LA 70803

Marcio de Queiroz[1]
Department of Mechanical and Industrial Engineering,
Louisiana State University,
Baton Rouge, LA 70803
e-mail: mdeque1@lsu.edu

Xiaoyu Cai
R&D Laser Tracker,
FARO Technologies,
Exton, PA 19341

Three-Dimensional Dynamic Formation Control of Multi-Agent Systems Using Rigid Graphs

In this paper, we consider the problem of formation control of multi-agent systems in three-dimensional (3D) space, where the desired formation is dynamic. This is motivated by applications where the formation size and/or geometric shape needs to vary in time. Using a single-integrator model and rigid graph theory, we propose a new control law that exponentially stabilizes the origin of the nonlinear, interagent distance error dynamics and ensures tracking of the desired, 3D time-varying formation. Extensions to the formation maneuvering problem and double-integrator model are also discussed. The formation control is illustrated with a simulation of eight agents forming a dynamic cube.
[DOI: 10.1115/1.4030973]

1 Introduction

A multi-agent system is a network of mobile physical entities (e.g., autonomous vehicles) that collectively perform a complex task beyond their individual capabilities. Among the many coordination and cooperation problems for multi-agent systems (aggregation, consensus, social foraging, flocking, etc.) [1–3], we are interested here in the *formation* problem. Formation control refers to the behavior where a group of agents acquire and maintain a prescribed geometric shape in space.

The formation control problem is relatively straightforward to solve if the agents' global coordinates can be measured. However, a global positioning system (GPS), which is typically used in such cases, has limited accuracy when there is no line of sight between the GPS receiver and satellite. Therefore, we consider the problem where each agent has only locally sensed information about the other agents from onboard sensors (e.g., inertial-type navigation system, laser range finder, camera, and/or compass).

Graph theory is a natural tool for modeling the multi-agent formation shape. *Rigid* graph theory, in particular, naturally ensures that the interagent distance constraints of the desired formation are enforced through the rigidity of the underlying graph. This implicitly guarantees that collisions between agents are avoided while acquiring the formation. Another advantage of using the interagent distances as the controlled variables is that position measurements in a global coordinate frame are not required [4] as would be the case when employing consensus-type algorithms [2] (see Ref. [5] for an overview of rigid graph theory and its application to sensing, communication, and control architectures for formations of autonomous vehicles).

Several results dealing with formation control based on stabilizing the interagent distance dynamics have appeared in the literature. For the case where the desired formation is planar two-dimensional (2D), formation controllers were proposed in Refs. [4,6–10] using the single-integrator model for the agents' motion, and in Ref. [11] for the double-integrator model. The extension to 3D formations using single- and double-integrator models was considered in Ref. [12]. In Refs. [13,14], 2D formation maneuvering[2] controllers were presented using the single-integrator model. Two-dimensional formation maneuvering and target interception schemes were designed using the single-integrator model in Refs. [1,15] and using the double-integrator model in Ref. [16].

In all the distance-based formation controllers described previously, the desired formation is *static* in the sense that its shape and size are fixed in time. In certain applications, it is necessary that the prescribed formation be *dynamic* in nature (size and/or shape is time varying). A typical example is when the multi-agent system needs to move through a narrow space while maintaining the formation shape. Therefore, in this paper, we extend the graph rigidity-based approach to the dynamic formation problem in 3D using the single-integrator model. We assume the desired formation is constructed to be infinitesimally and minimally rigid for all time. Using Lyapunov-based arguments, we design a formation controller to exponentially stabilize the dynamics of the interagent distance errors and track the desired formation while avoiding ambiguous formations. We then present two extensions to the control law: how to perform formation maneuvering on top of tracking the time-varying formation, and how to account for double-integrator modeled agents.

The paper is organized as follows: In Sec. 2, we introduce some relevant concepts of rigid graph theory in $\mathbb{R}^3$. The problem statement is given in Sec. 3. In Sec. 4, we present the single-integrator formation control law and closed-loop stability analysis. The extensions to formation maneuvering and double-integrator dynamics are discussed in Sec. 5. Simulation results are shown in Sec. 6. Finally, concluding remarks are made in Sec. 7.

2 Notation and Basic Concepts

Throughout the paper, the following notation is used: $x \in \mathbb{R}^m$ or $x = [x_1, \ldots, x_m]$ denotes an $m \times 1$ vector; $x = [x_1, \ldots, x_m]$ where $x_i \in \mathbb{R}^n$ denotes an $nm \times 1$ vector; $\|x\|$ denotes the Euclidean norm; dist $(\zeta, \mathcal{M}) := \inf_{x \in \mathcal{M}} \|\zeta - x\|$ for points $\zeta, x \in \mathbb{R}^m$ and set $\mathcal{M}$; and $\mathbf{1}_m$ is the $m \times 1$ vector of ones.

An undirected graph G is a pair (V, E), where $V = \{1, 2, \ldots, n\}$ is the set of vertices, $E = \{(i,j) : i,j \in V, i \neq j\}$ is the set of undirected edges where there is no distinction between (i, j) and (j, i), and $l \in \{1, \ldots, n(n-1)/2\}$ is the number of edges in E. If $p_i \in \mathbb{R}^3$ is the coordinate of vertex i, then a framework F is a pair (G, p) where $p = [p_1, \ldots, p_n] \in \mathbb{R}^{3n}$.

The edge function $\phi : \mathbb{R}^{3n} \to \mathbb{R}^l$ is defined as

$$\phi(p) = \left[\ldots, \left\|p_i - p_j\right\|^2, \ldots\right], \quad (i,j) \in E \tag{1}$$

where the kth component, $\left\|p_i - p_j\right\|^2$, corresponds to the kth edge in E connecting vertices i and j. The rigidity matrix $R : \mathbb{R}^{3n} \to \mathbb{R}^{l \times 3n}$ of $F = (G, p)$ is defined as

$$R(p) = \frac{1}{2}\frac{\partial \phi(p)}{\partial p} \tag{2}$$

It is known that rank $[R(p)] \leq 3n - 6$ [17].

[1]Corresponding author.

Contributed by the Dynamic Systems Division of ASME for publication in the JOURNAL OF DYNAMIC SYSTEMS, MEASUREMENT, AND CONTROL. Manuscript received January 21, 2015; final manuscript received June 5, 2015; published online August 13, 2015. Assoc. Editor: Sergey Nersesov.

[2]In formation maneuvering, the agents simultaneously acquire a formation and translate cohesively as a rigid body following a given trajectory.

An isometry of $\mathbb{R}^3$ is a bijective map $T:\mathbb{R}^3 \to \mathbb{R}^3$ satisfying [18]

$$\|x-y\| = \|T(x)-T(y)\|, \quad \forall x,y \in \mathbb{R}^3 \tag{3}$$

The transformation T accounts for rotation and translation of the vector $x-y$. Two frameworks are said to be *isometric* in $\mathbb{R}^3$ if they are related by an isometry in $\mathbb{R}^3$. We denote the set of all frameworks that are isometric to F by Iso (F). Note that Eq. (1) is invariant under isometric motions of F [5,9,19].

Frameworks (G, p) and $(G, \hat{p})$ are said to be equivalent if $\phi(p)=\phi(\hat{p})$, and congruent if $\|p_i-p_j\| = \|\hat{p}_i-\hat{p}_j\|$ for all $i,j \in V$ [20]. A framework (G, p), where $n>3$ and p is generic,[3] is infinitesimally rigid if and only if rank $[R(p)] = 3n-6$ [18]. An infinitesimally rigid framework (G, p) is minimally rigid if and only if $l = 3n-6$ [5]. If two infinitesimally rigid frameworks (G,p) and $(G,\hat{p})$ are equivalent but not congruent, they are called *ambiguous* [5]. We denote the set of all frameworks that are ambiguous to an infinitesimally rigid framework F by Amb(F). We assume that all the frameworks in Amb(F) are also infinitesimally rigid. This assumption is reasonable and, in fact, holds almost everywhere; see Ref. [5] and Theorem 3 of Ref. [22] for details.

3 Problem Statement

Consider a system of n kinematic agents in space modeled by the single integrator

$$\dot{q}_i = u_i, \quad i=1,\ldots,n \tag{4}$$

where $q_i = [x_i, y_i, z_i] \in \mathbb{R}^3$ is the position and $u_i \in \mathbb{R}^3$ is the (velocity-level) control input of the ith agent with respect to an earth-fixed coordinate frame.

Let the desired formation for the agents be represented by a *dynamic*, infinitesimally, and minimally rigid framework $F^*(t) = (G^*, q^*(t))$, where $G^* = (V^*, E^*)$, dim $(V^*)=n$, dim $(E^*)=l$, and $q^* = [q_1^*,\ldots,q_n^*]$. The time-varying desired distance between agents i and j is given by

$$d_{ij}(t) = \left\| q_i^*(t) - q_j^*(t) \right\| > 0, \quad i,j \in V^* \tag{5}$$

We assume the desired distances are such that d_{ij} and $\dot{d}_{ij}$ are bounded continuous functions of time.

Consider that the actual formation of the agents is represented by the framework $F(t) = (G^*, q(t))$ where $q=[q_1,\ldots,q_n]$. Assume that the relative position of agent pairs in E^* can be measured. Further, assume that at $t=0$ the agents do not satisfy the desired interagent distance constraints, i.e., $\|q_i(0)-q_j(0)\| \neq d_{ij}(0), i,j \in V^*$.

Our control objective is to design $u_i = u_i(q_i-q_j, d_{ij}, \dot{d}_{ij})$, $i=1,\ldots,n$ and $(i,j) \in E^*$ such that

$$F(t) - \text{Iso}\ (F^*(t)) \to 0 \text{ as } t \to \infty \tag{6}$$

or equivalently

$$\left\|q_i(t)-q_j(t)\right\| - d_{ij}(t) \to 0 \text{ as } t\to\infty, \quad i,j \in V^* \tag{7}$$

4 Formation Control Design

We begin by defining the relative position of two agents as

$$\tilde{q}_{ij} = q_i - q_j, \quad (i,j) \in E^* \tag{8}$$

and the distance tracking error as

$$e_{ij} = \left\|\tilde{q}_{ij}\right\| - d_{ij}, \quad (i,j) \in E^* \tag{9}$$

The distance tracking error dynamics can be derived from Eqs. (9) and (4) as

$$\dot{e}_{ij} = \left(\tilde{q}_{ij}^\top \tilde{q}_{ij}\right)^{-\frac{1}{2}} \tilde{q}_{ij}^\top (u_i - u_j) - \dot{d}_{ij} = \frac{\tilde{q}_{ij}^\top (u_i-u_j)}{e_{ij}+d_{ij}} - \dot{d}_{ij} \tag{10}$$

Let

$$z_{ij} = \left\|\tilde{q}_{ij}\right\|^2 - d_{ij}^2, \quad (i,j) \in E^* \tag{11}$$

which can be rewritten as

$$z_{ij} = e_{ij}(e_{ij} + 2d_{ij}) \tag{12}$$

using Eq. (9). Given that $\|\tilde{q}_{ij}\| \geq 0$, it is not difficult to check that $z_{ij}=0$ if and only if $e_{ij}=0$. Now, define the following Lyapunov function candidate:

$$W(e) = \frac{1}{4}\sum_{(i,j)\in E^*} z_{ij}^2 \tag{13}$$

where $e = [\ldots, e_{ij}, \ldots] \in \mathbb{R}^l, (i,j) \in E^*$ is ordered as Eq. (1). This function is positive definite in e and its level surfaces, $W(e)=c$ for some $c>0$, are closed since $e_{ij} \geq -d_{ij}$.

Differentiating Eq. (13) along Eq. (10) gives

$$\dot{W} = \sum_{(i,j)\in E^*} e_{ij}(e_{ij}+2d_{ij}) \left[\tilde{q}_{ij}^\top (u_i-u_j) - d_{ij}\dot{d}_{ij}\right] \tag{14}$$

Using Eqs. (2) and (12), Eq. (14) can be conveniently written as

$$\dot{W} = z^\top (R(q)u - d_v) \tag{15}$$

where $u=[u_1,\ldots,u_n] \in \mathbb{R}^{3n}, z = [\ldots, z_{ij}, \ldots] \in \mathbb{R}^l, d_v = [\ldots, d_{ij}\dot{d}_{ij}, \ldots] \in \mathbb{R}^l, (i,j) \in E^*$, and the elements in z and d_v are ordered as Eq. (1).

Before presenting the main result, we state the following lemmas since they will be useful in establishing the closed-loop stability set with respect to the infinitesimal rigidity and ambiguities of the framework modeling the formation.

Lemma 1. *Consider two frameworks $F=(G,p)$ and $\bar{F}=(G,\bar{p})$ sharing the same graph $G=(V,E)$ and the function [11]*

$$\Psi(\bar{F}, F) = \sum_{(i,j)\in E} \left(\|\bar{p}_i - \bar{p}_j\| - \|p_i - p_j\|\right)^2 \tag{16}$$

If F is infinitesimally rigid and $\Psi(\bar{F},F) \leq \delta$, where δ is a sufficiently small positive constant, then $\bar{F}$ is also infinitesimally rigid.

Lemma 2. *For non-negative constants c and δ, the level set $W(e) \leq c$ is equivalent to $\Psi(F,F^*) \leq \delta$, where W and Ψ were defined in Eqs. (13) and (16), respectively [11].*

The theorem below gives the formation tracking control law.

Theorem 1. *Consider the formation $F(t) = (G^*, q(t))$, and let the initial conditions of the error dynamics be such that $e(0) \in \Omega_1 \cap \Omega_2$ where*

$$\begin{aligned} \Omega_1 &= \left\{e \in \mathbb{R}^l | \Psi(F,F^*) \leq \delta\right\}, \\ \Omega_2 &= \left\{e \in \mathbb{R}^l | \text{dist}(q, \text{Iso}(F^*)) < \text{dist}(q, \text{Amb}(F^*))\right\} \end{aligned} \tag{17}$$

and δ is a sufficiently small positive constant. The control law

$$u = R^+(q)(-k_v z + d_v) \tag{18}$$

[3]By generic, we mean the affine span of p is all of $\mathbb{R}^m$ [21].

where $R^{+}(q) = R^{\top}(q)[R(q)R^{\top}(q)]^{-1}$ is the Moore–Penrose pseudoinverse and $k_v > 0$ yields $e = 0$ exponentially stable and guarantees that Eq. (6) is satisfied.

Proof. Given that $F^*(t)$ and $F(t)$ have the same number of edges and $F^*(t)$ is minimally rigid for all time, then $F(t)$ is minimally rigid for all $t \geq 0$. Since $F^*(t)$ is infinitesimally rigid for all time, we know from Lemma 1 that $F(t)$ is infinitesimally rigid for $e(t) \in \Omega_1 \cap \Omega_2$. Since $F(t)$ is infinitesimally and minimally rigid for $e(t) \in \Omega_1 \cap \Omega_2$, then $R(q)$ has full row rank and $R(q)R^{+}(q) = I$ [23] for $e(t) \in \Omega_1 \cap \Omega_2$. Therefore, substituting Eq. (18) into Eq. (15) yields

$$\dot{W} = -k_v z^{\top} z = -4k_v W \quad \text{for} \quad e(t) \in \Omega_1 \cap \Omega_2 \tag{19}$$

where Eq. (13) was used. From Eq. (19), we know that $\dot{W}(t) \leq 0$ for all $t \geq 0$; hence, $W(t)$ is decreasing or constant for all $t \geq 0$. Then, since $e(t) \in \Omega_1$ is equivalent to $e(t) \in \{e \in \mathbb{R}^l | W(e) \leq c\}$ from Lemma 2, a sufficient condition for Eq. (19) is given by

$$\dot{W} \leq -4k_v W \quad \text{for} \quad e(0) \in \Omega_1 \cap \Omega_2 \tag{20}$$

From the form of Eq. (20), we can conclude that $e = 0$ is exponentially stable for $e(0) \in \Omega_1 \cap \Omega_2$ [24].

The exponential stability of $e = 0$ indicates that $F(t) -$ Iso $(F^*(t)) \to 0$ or $F(t) -$ Amb $(F^*(t)) \to 0$ as $t \to \infty$. Now, since $e(0) \in \Omega_1 \cap \Omega_2$, we have from Eq. (17) that

$$\text{dist}(q(0), \text{Iso}(F^*(0))) < \text{dist}(q(0), \text{Amb}(F^*(0))) \tag{21}$$

Due to Eq. (21), the energylike function $W(t)$ would need to increase for a period of time for $F(t) -$ Amb $(F^*(t)) \to 0$ as $t \to \infty$, which is a contradiction since Eq. (20) establishes that $W(t)$ is decreasing or constant for all $t \geq 0$. Therefore, we know $F(t) -$ Iso $(F^*(t)) \to 0$ as $t \to \infty$ for $e(0) \in \Omega_1 \cap \Omega_2$.

Remark 1. The initial condition $e(0) \in \Omega_1 \cap \Omega_2$ in Theorem 1 is a sufficient condition for the actual formation $F(t)$ to satisfy two constraints: (a) remain infinitesimally rigid for all time and (b) be closer to a framework in Iso (F^*) at $t = 0$ than to one in Amb (F^*) in order to avoid converging to an ambiguous framework. The former constraint is satisfied by $e(0) \in \Omega_1$, while the latter is satisfied by $e(0) \in \Omega_2$. The set $\Omega_1 \cap \Omega_2$ exists because it is always possible to select $F(0)$ in the above-described manner.

5 Extensions

5.1 Formation Maneuvering. One can modify the control law (18) to include a formation maneuvering term to allow the swarm to move cohesively (as a rigid body) with a given translational velocity while tracking the desired formation. Specifically, we can set

$$u = R^{+}(q)(-k_v z + d_v) + (\mathbf{1}_n \otimes v_d) \tag{22}$$

where $v_d \in \mathbb{R}^3$ is any bounded, continuous function of time representing the desired translational velocity for the swarm, and $\otimes$ is the Kronecker product.

Note that the formation maneuvering term $\mathbf{1}_n \otimes v_d$ does not affect the formation tracking analysis in Theorem 1. That is, substituting Eq. (22) into Eq. (15) still gives Eq. (20) since $R(q)(\mathbf{1}_n \otimes v_d) = 0$. To see this, observe from Eq. (2) that each row of the rigidity matrix $R(q)$ takes the form

$$\left[0 \ldots 0 \ (q_i - q_j)^{\top} 0 \ldots 0 \ (q_j - q_i)^{\top} 0 \ldots 0\right] \tag{23}$$

Thus, the product of each $1 \times 3n$ row of $R(q)$ with the $3n \times 1$ vector $\mathbf{1}_n \otimes v_d$ will be

$$(q_i - q_j)^{\top} v_d + (q_j - q_i)^{\top} v_d = 0 \tag{24}$$

5.2 Double-Integrator Model. The control formulation in Sec. 5.1 can be extended to the double-integrator model

$$\begin{aligned} \dot{q}_i &= v_i \\ \dot{v}_i &= u_i, \quad i = 1, \ldots, n \end{aligned} \tag{25}$$

where $v_i \in \mathbb{R}^3$ represents the ith agent velocity and $u_i \in \mathbb{R}^3$ is the acceleration-level control input for the ith agent. This extension is rather seamless if one exploits the integrator backstepping technique [25], since the only difference between Eqs. (4) and (25) is an additional integrator. Here, we need to assume the desired distances defined in Eq. (5) are such that $d_{ij}, \dot{d}_{ij},$ and $\ddot{d}_{ij}$ are bounded continuous functions, and that $v_d, \dot{v}_d$ are bounded and continuous.

COROLLARY 1. *The control*

$$u = -k_a s + \dot{v}_f - R^{\top}(q) z \tag{26}$$

where $k_a > 0$, $s = v - v_f, v = [v_1, \ldots, v_n] \in \mathbb{R}^{3n}$, and $v_f \in \mathbb{R}^{3n}$ is equal to the right-hand side of Eq. (22), renders $(e, s) = 0$ exponentially stable and ensures that Eq. (6) is satisfied for initial conditions $(e(0), s(0)) \in (\Omega_1 \cap \Omega_2) \times \mathbb{R}^{3n}$.

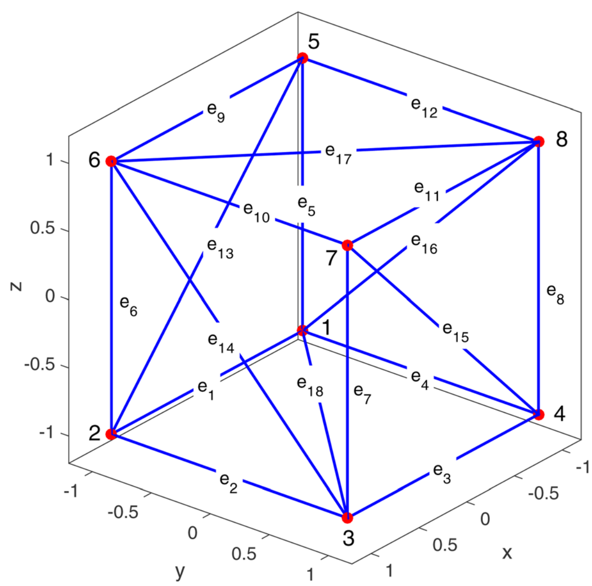

Fig. 1 Desired formation $F^*(t)$ at $t = 0$

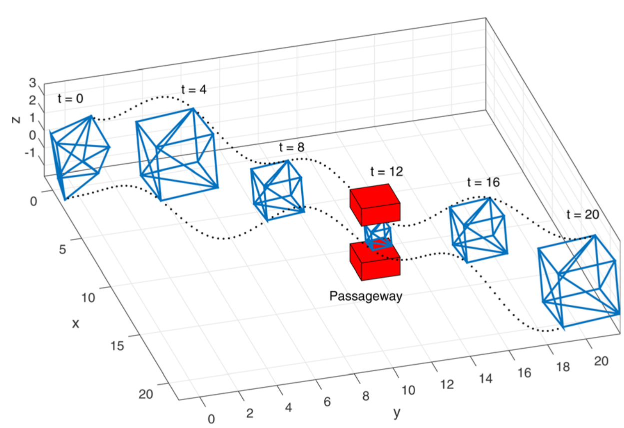

Fig. 2 Single-integrator: agent trajectories from an arbitrary initial formation

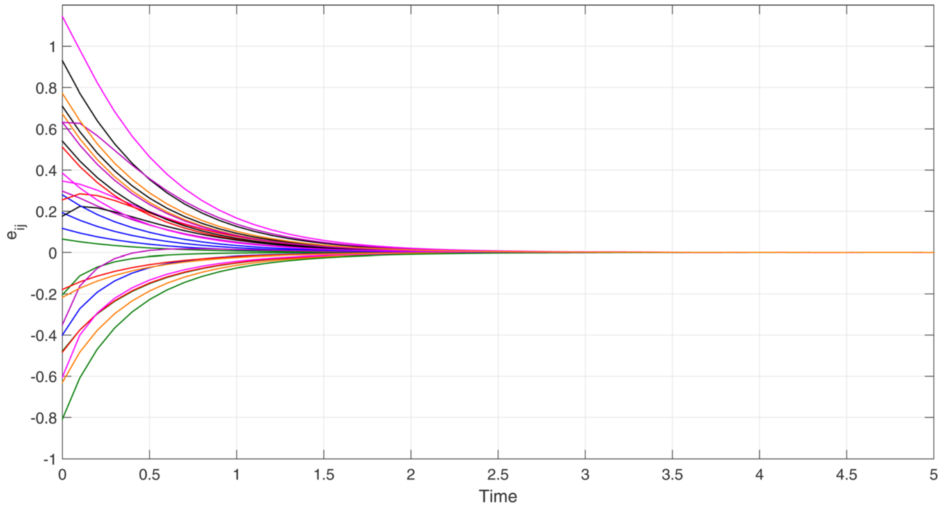

Fig. 3 Single-integrator: interagent distance errors for $i, j \in V^*$

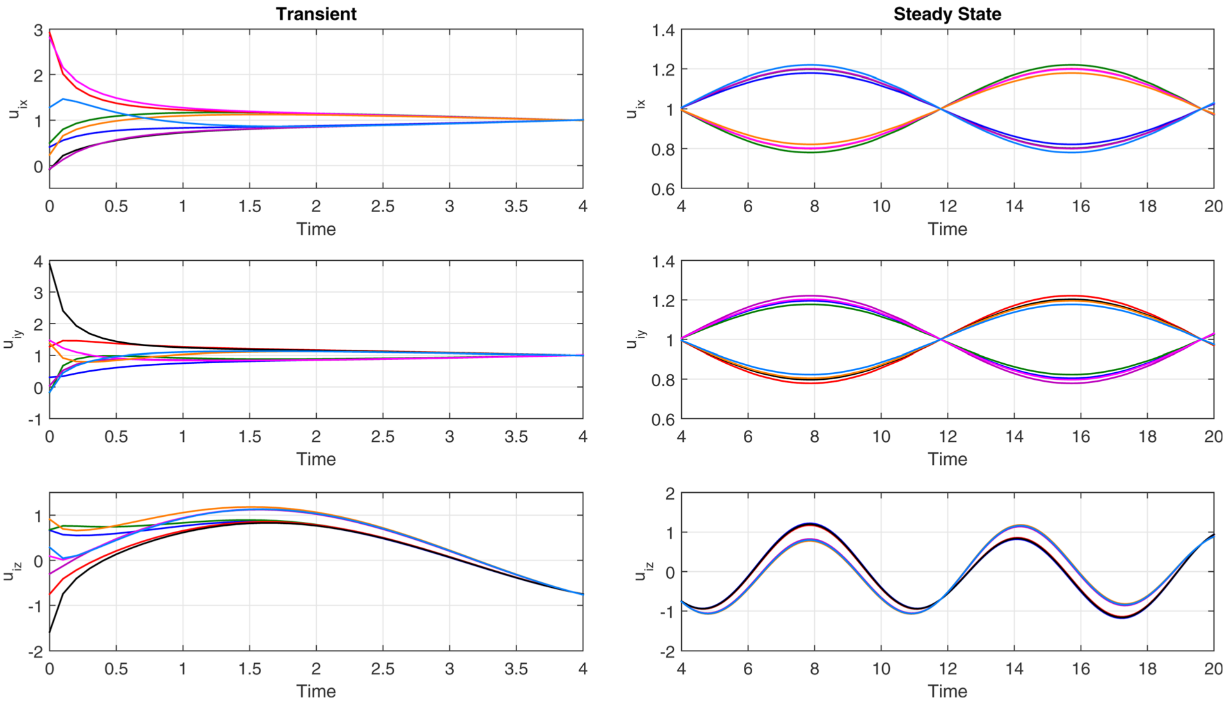

Fig. 4 Single-integrator: control inputs along x (top plot), y (middle plot), and z (bottom plot) directions for $i = 1, \ldots, 8$ during the transient phase (left plots) and steady-state phase (right plots)

Sketch of Proof. We only show the key parts of the proof since it follows from similar arguments used in Theorem 1. We start with the Lyapunov function candidate

$$W_d(e, s) = W(e) + \frac{1}{2} s^\top s \tag{27}$$

where W was defined in Eq. (13) and the variable s quantifies the error between the actual velocity and the "virtual" velocity input v_f. After taking the time derivative of Eq. (27), we obtain

$$\dot{W}_d = z^\top \left(R(q)v_f - d_v\right) + s^\top \left(u + R^\top(q)z - \dot{v}_f\right) \tag{28}$$

where Eq. (25) and the definition of s were used. Substituting Eq. (26) and v_f into Eq. (28) yields

$$\dot{W}_d = -k_v z^\top z - k_a s^\top s \leq -2 \min(k_v, k_a) W_d \quad \text{for} \quad (e(t), s(t)) \in (\Omega_1 \cap \Omega_2) \times \mathbb{R}^{3n} \tag{29}$$

from which we can conclude that $(e, s) = 0$ is exponentially stable for $(e(0), s(0)) \in (\Omega_1 \cap \Omega_2) \times \mathbb{R}^{3n}$. The proof of Eq. (6) proceeds as in the proof of Theorem 1.

Remark 2. The term $\dot{v}_f$ in Eq. (26) can be explicitly calculated as follows:

$$\dot{v}_f = \dot{R}^+(q)(-k_v z + d_v) + R^+(q)\left(-k_v \dot{z} + \dot{d}_v\right) + (\mathbf{1}_n \otimes \dot{v}_d) \tag{30}$$

where

$$\dot{z} = 2(R(q)v - d_v) \tag{31}$$

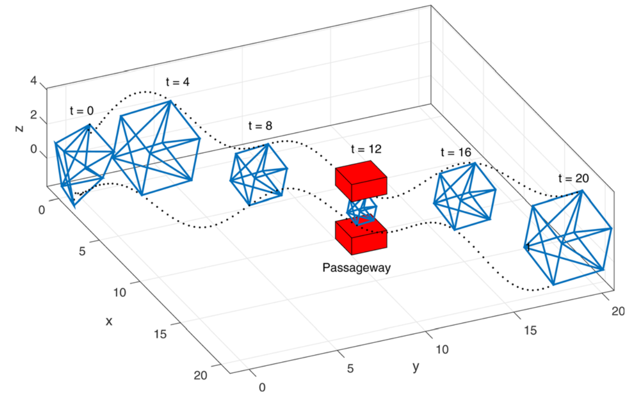

Fig. 5 Double-integrator: agent trajectories from an arbitrary initial formation

$$\dot{d}_v = \left[\dots, \dot{d}_{ij}^2 + d_{ij}\ddot{d}_{ij}, \dots \right], \quad (i,j) \in E^* \tag{32}$$

$$\dot{R}^+ = \dot{R}^\top \left(RR^\top\right)^{-1} - R^\top \left(RR^\top\right)^{-1} \frac{d\left(RR^\top\right)}{dt} \left(RR^\top\right)^{-1} \tag{33}$$

and $\dot{R}(q) = R(v)$. It is important to point out that the terms $R(q)v$ and $\dot{R}(q)$ are only a function of $q_i - q_j$ and $v_i - v_j$ for $(i,j) \in E^*$. As a result, Eq. (30) is only a function of $q_i - q_j, v_i - v_j$, d_{ij}, $\dot{d}_{ij}, \ddot{d}_{ij}$, and $\dot{v}_d$ for $(i,j) \in E^*$, while the ith component of Eq. (26) is a function of these variables as well as v_i and v_d.

6 Simulation Results

A simulation with eight agents was performed to demonstrate the proposed formation control laws. We simulated a scenario where the formation needs to change in order to go through a narrow passageway. To this end, the desired dynamic formation $F^*(t)$ was set to a cube that expanded and contracted uniformly

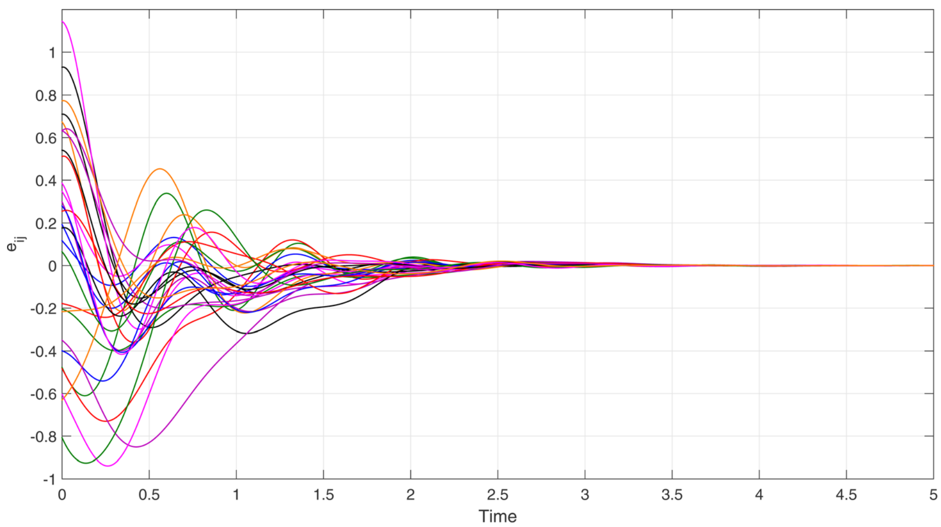

Fig. 6 Double-integrator: interagent distance error for $i, j \in V^*$

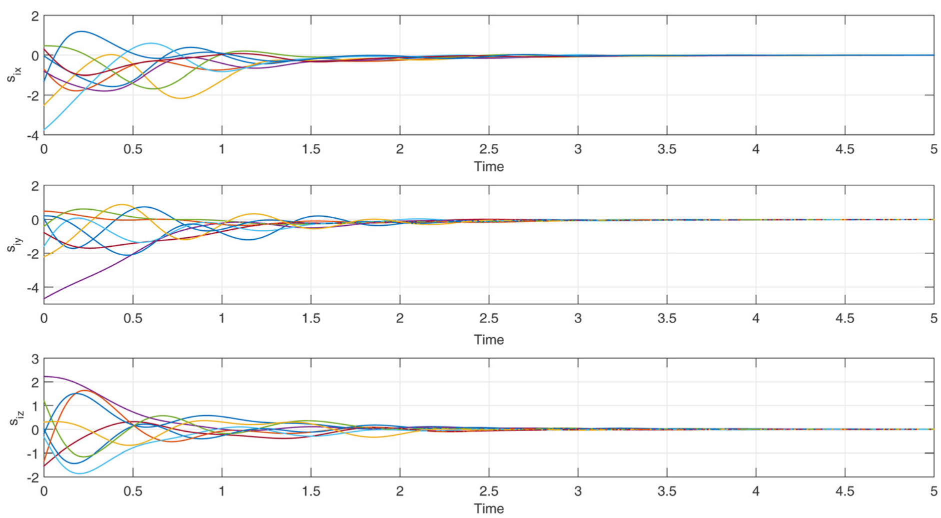

Fig. 7 Double-integrator: variable s along x (top plot), y (middle plot), and z (bottom plot) directions for $i = 1, \dots, 8$

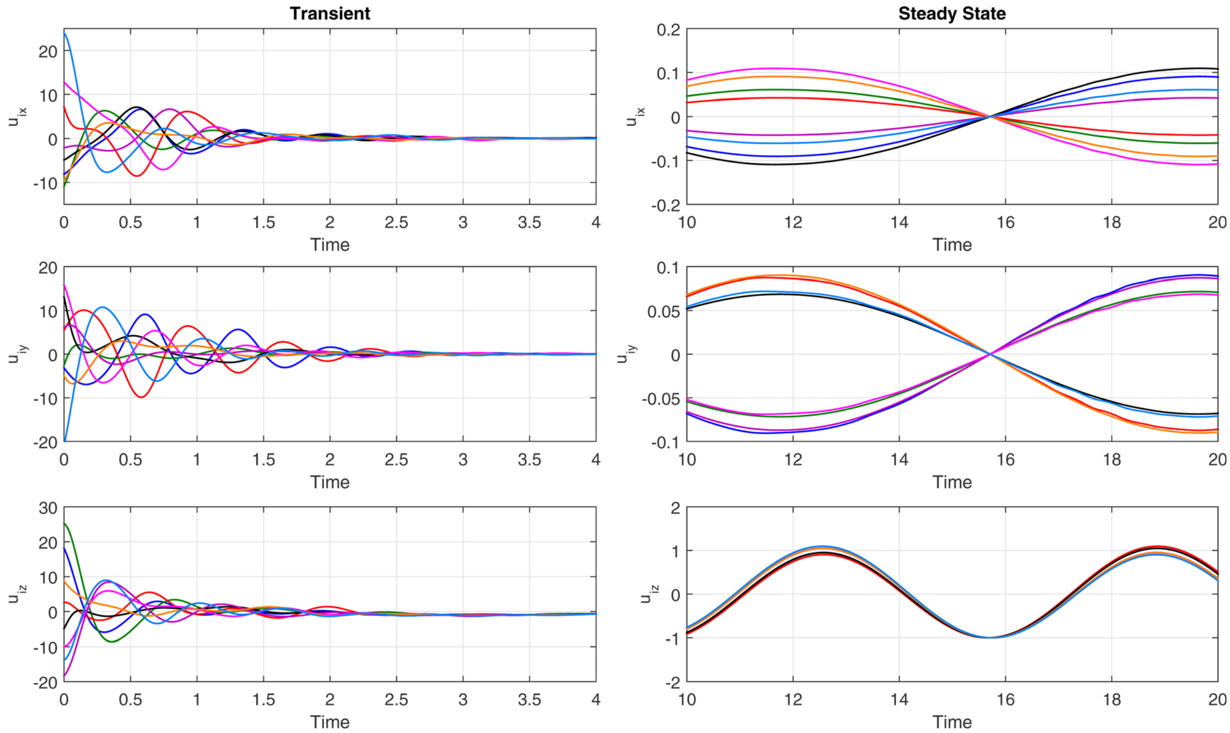

Fig. 8 Double-integrator: control inputs along *x* (top plots), *y* (middle plots), and *z* (bottom plots) directions for $i = 1, \ldots, 8$ during the transient phase (left plots) and steady-state phase (right plots)

over time.[4] Figure 1 shows $F^*(t=0)$ with vertices at $q_1^*(0) = [-1,-1,-1], q_2^*(0) = [1,-1,-1], q_3^*(0) = [1,1,-1], q_4^*(0) = [-1,1,-1]$, $q_5^*(0) = [-1,-1,1]$, $q_6^*(0) = [1,-1,1]$, $q_7^*(0) = [1,1,1]$, and $q_8^*(0) = [-1,1,1]$. The desired framework was made minimally rigid and infinitesimally rigid by introducing the 18 edges labeled as e_i, $i = 1, \ldots, 18$ in Fig. 1. The desired formation was made dynamic by setting

$$q_i^*(t) = q_i^*(0)(1 + 0.5 \sin 0.4t), \quad i = 1, \ldots, 8 \tag{34}$$

As a result, the desired distances between the agents were given by $d_{12}(t) = d_{23}(t) = d_{34}(t) = d_{45}(t) = d_{15}(t) = d_{26}(t) = d_{37}(t) = d_{48}(t) = d_{56}(t) = d_{67}(t) = d_{58}(t) = d_{78}(t) = 2 + \sin 0.4t$ and $d_{13}(t) = d_{18}(t) = d_{25}(t) = d_{36}(t) = d_{47}(t) = d_{68}(t) = 2\sqrt{2} + \sqrt{2} \sin 0.4t$.

6.1 Single-Integrator Result. For the single-integrator model, the control law (22) was simulated since it includes Eq. (18). The desired swarm velocity was set to

$$v_d = [1, 1, \sin t] \tag{35}$$

The initial conditions of the agents were selected according to

$$q_i(0) = q_i^*(0) + \text{rand}\ (3) - 0.5\mathbf{1}_3 \tag{36}$$

where rand(3) generates a random 3×1 vector, whose elements are uniformly distributed on the interval (0, 1). The control gain k_v in Eq. (22) was set to 1.

Figure 2 shows the agent trajectories over time as they track the desired dynamic formation while translating according to Eq. (35). By the $t = 4$ snapshot, the cubic formation is already acquired. Figure 3 shows all interagent distance errors $e_{ij}(t), i,j \in V^*$ converging to zero at about $t = 4$. The *x*-, *y*-, and *z*-direction components of the control inputs $u_i(t), i = 1, \ldots, 8$ are given in Fig. 4, where for ease of visualization they are separated into transient and steady-state phases. Notice that the control inputs for each direction converge to the corresponding component of Eq. (35) plus the contribution of Eq. (34) to each agent velocity.

6.2 Double-Integrator Result. We then simulated the control law (26) for the double-integrator model. The desired swarm velocity was set to Eq. (35) with the corresponding desired swarm acceleration being

$$\dot{v}_d = [0, 0, \cos t] \tag{37}$$

The initial positions of agents were selected as in Eq. (36), while their initial velocities were given by

$$v_i(0) = 2(\text{rand}(3) - 0.5\mathbf{1}_3) \tag{38}$$

The control gains in Eq. (26) were set to $k_v = k_a = 1$.

Figure 5 shows the time snapshots of the agent trajectories. Figure 6 shows all interagent distance errors converging to zero, where the oscillations are due to the second-order nature of the double-integrator dynamics. In Fig. 7, we show the *x*-, *y*-, and *z*-direction components of the agent velocity error $s_i(t)$, $i = 1, \ldots 8$. The components of the acceleration-level control inputs $u_i(t)$ are given in Fig. 8.

7 Conclusions

We constructed new 3D formation control laws for stabilizing interagent distances to predefined, time-varying values using the single- and double-integrator models. The controller only requires measurement of the relative position of agents connected in the infinitesimally and minimally rigid graph modeling the desired dynamic formation. A Lyapunov-like analysis was used to prove the exponentially stability of the origin of the distance error dynamics and tracking of the desired formation. Sufficient conditions

[4]In practice, $F^*(t)$ would be generated online by a path planning module that includes a perceptive model of the environment.

for avoiding convergence to ambiguous formations were given in the stability analysis. We also showed how the control can be augmented with a term that allows the dynamic formation to maneuver as a rigid body with a given translational velocity.

References

[1] Gazi, V., and Passino, K. M., 2011, *Swarm Stability and Optimization*, Springer-Verlag, Berlin.
[2] Ren, W., and Beard, R. W., 2008, *Distributed Consensus in Multi-Vehicle Cooperative Control*, Springer-Verlag, London.
[3] Ren, W., and Cao, Y., 2011, *Distributed Coordination of Multi-Agent Networks: Emergent Problems, Models, and Issues*, Springer-Verlag, London.
[4] Summers, T. H., Yu, C., Dasgupta, S., and Anderson, B. D. O., 2011, "Control of Minimally Persistent Leader-Remote-Follower and Coleader Formations in the Plane," IEEE Trans. Autom. Control, **56**(12), pp. 2778–2792.
[5] Anderson, B. D. O., Yu, C., Fidan, B., and Hendrickx, J. M., 2008, "Rigid Graph Control Architectures for Autonomous Formations," IEEE Control Syst. Mag., **28**(6), pp. 48–63.
[6] Cai, X., and de Queiroz, M., 2012, "On the Stabilization of Planar Multi-Agent Formations," ASME Paper No. DSCC2012-MOVIC2012-8534.
[7] Cao, M., Morse, A. S., Yu, C., Anderson, B. D. O., and Dasgupta, S., 2011, "Maintaining a Directed, Triangular Formation of Mobile Autonomous Agents," Commun. Inf. Syst., **11**(1), pp. 1–16.
[8] Dörfler, F., and Francis, B., 2010, "Geometric Analysis of the Formation Problem for Autonomous Robots," IEEE Trans. Autom. Control, **55**(10), pp. 2379–2384.
[9] Krick, L., Broucke, M. E., and Francis, B. A., 2009, "Stabilization of Infinitesimally Rigid Formations of Multi-Robot Networks," Int. J. Control, **82**(3), pp. 423–439.
[10] Oh, K.-K., and Ahn, H.-S., 2011, "Formation Control of Mobile Agents Based on Inter-Agent Distance Dynamics," Automatica, **47**(10), pp. 2306–2312.
[11] Cai, X., and de Queiroz, M., 2014, "Rigidity-Based Stabilization of Multi-Agent Formations," ASME J. Dyn. Syst., Meas., Control, **136**(1), p. 014502.
[12] Oh, K.-K., and Ahn, H.-S., 2014, "Distance-Based Undirected Formations of Single-Integrator and Double-Integrator Modeled Agents in *n*-Dimensional Space," Int. J. Robust Nonlinear Control, **24**(12), pp. 1809–1820.
[13] Kang, S.-M., Park, M.-C., Lee, B.-H., and Ahn, H.-S., 2014, "Distance-Based Formation Control With a Single Moving Leader," American Control Conference (ACC), Portland, OR, June 4–6, pp. 305–310.
[14] Oh, K.-K., and Ahn, H.-S., 2011, "Distance-Based Control of Cycle-Free Persistent Formations," IEEE International Symposium on Intelligent Control (ISIC), Denver, CO, Sept. 28–30, pp. 816–821.
[15] Cai, X., and de Queiroz, M., 2013, "Multi-Agent Formation Maintenance and Target Tracking," American Control Conference (ACC), Washington, DC, June 17–19, pp. 2537–2532.
[16] Cai, X., and de Queiroz, M., 2015, "Formation Maneuvering and Target Interception for Multi-Agent Systems Via Rigid Graphs," Asian J. Control, **17**(6), pp. 1–13.
[17] Asimow, L., and Roth, B., 1979, "The Rigidity of Graphs, II," J. Math. Anal. Appl., **68**(1), pp. 171–190.
[18] Izmestiev, I., 2009, *Infinitesimal Rigidity of Frameworks and Surfaces* (Lectures on Infinitesimal Rigidity), Kyushu University, Fukuoka, Japan.
[19] Roth, B., 1981, "Rigid and Flexible Frameworks," Am. Math. Monthly, **88**(1), pp. 6–21.
[20] Jackson, B., 2007, "Notes on the Rigidity of Graphs," Levico Conference Notes, Levico Terme, Italy, Oct. 22–26.
[21] Connelly, R., 2005, "Generic Global Rigidity," Discrete Comput. Geom., **33**(4), pp. 549–563.
[22] Aspnes, J., Egen, T., Goldenberg, D. K., Morse, A. S., Whiteley, W., Yang, Y. R., Anderson, B. D. O., and Belhumeur, P. N., 2006, "A Theory of Network Localization," IEEE Trans. Mobile Comput., **5**(12), pp. 1663–1678.
[23] Ben-Israel, A., and Greville, T. N. E., 2003, *Generalized Inverses: Theory and Applications*, Springer-Verlag, New York.
[24] Khalil, H. K., 2002, *Nonlinear Systems*, Prentice Hall, Englewood Cliffs, NJ.
[25] Krstic, M., Kanellakopoulos, I., and Kokotovic, P., 1995, *Nonlinear and Adaptive Control Design*, Wiley, New York.